

UC Office of the President

Recent Work

Title

Model to explain the behavior of 2DEG mobility with respect to charge density in N-polar and Ga-polar AlGa_N-Ga_N heterostructures

Permalink

<https://escholarship.org/uc/item/4k6287tr>

Journal

Journal of Applied Physics, 120(11)

Author

Ahmadi, Elaheh

Publication Date

2016-09-21

Peer reviewed

Model to explain the behavior of 2DEG mobility with respect to charge density in N-polar and Ga-polar AlGa_N-Ga_N heterostructures

Elaheh Ahmadi, Stacia Keller, and Umesh K. Mishra

Citation: [Journal of Applied Physics](#) **120**, 115302 (2016); doi: 10.1063/1.4962321

View online: <http://dx.doi.org/10.1063/1.4962321>

View Table of Contents: <http://scitation.aip.org/content/aip/journal/jap/120/11?ver=pdfcov>

Published by the [AIP Publishing](#)

Articles you may be interested in

[Scattering induced by Al segregation in AlGa_N/Ga_N heterostructures](#)

Appl. Phys. Lett. **107**, 072105 (2015); 10.1063/1.4928932

[Temperature dependent effective mass in AlGa_N/Ga_N high electron mobility transistor structures](#)

Appl. Phys. Lett. **101**, 192102 (2012); 10.1063/1.4765351

[MBE growth of high electron mobility 2DEGs in AlGa_N/Ga_N heterostructures controlled by RHEED](#)

AIP Advances **2**, 012108 (2012); 10.1063/1.3679149

[Two dimensional electron gases induced by spontaneous and piezoelectric polarization in undoped and doped AlGa_N/Ga_N heterostructures](#)

J. Appl. Phys. **87**, 334 (2000); 10.1063/1.371866

[AlGa_N/Ga_N heterostructures on insulating AlGa_N nucleation layers](#)

Appl. Phys. Lett. **75**, 388 (1999); 10.1063/1.124384



NEW Special Topic Sections

NOW ONLINE
Lithium Niobate Properties and Applications:
Reviews of Emerging Trends

AIP | Applied Physics Reviews

Model to explain the behavior of 2DEG mobility with respect to charge density in N-polar and Ga-polar AlGa_N-Ga_N heterostructures

Elaheh Ahmadi, Stacia Keller, and Umesh K. Mishra

Department of Electrical and Computer Engineering, University of California, Santa Barbara, California 93106, USA

(Received 5 June 2016; accepted 24 August 2016; published online 16 September 2016)

There are three possible ways of reducing the charge density (n_s) in the N-polar high electron mobility transistors (HEMT) structures, by decreasing the channel thickness, applying reverse gate bias, or modifying the back-barrier. Understanding the behavior of 2DEG mobility as a function of n_s is essential to design high performance HEMT devices. Experimental data show that in the N-polar HEMT structures, the 2DEG mobility reduces as the n_s decreases by applying reverse gate bias or decreasing channel thickness, whereas in the Ga-polar HEMT structures, the 2DEG mobility increases as the n_s in the channel decreases by applying reverse gate bias. In this paper, the 2DEG mobility as a function of n_s is calculated in N-polar HEMTs for three different aforementioned cases, and is compared to that in the Ga-polar HEMT structures. It is shown that the conventional scattering mechanisms cannot explain these different behaviors. Two new scattering mechanisms, such as scattering from charged interface states and surface state dipoles (SSD), are introduced. It is revealed that in N-polar HEMT structures, reducing n_s by applying reverse gate bias or decreasing channel thickness moves the charge centroid closer to the AlGa_N-Ga_N interface. A combination of lower charge density (less screening of the scattering potential) and smaller distance between charge centroid and charged states at the interface leads to a severe mobility degradation in these cases. In contrast, reducing n_s by modifying the back-barrier (decreasing back-barrier doping and/or decreasing AlGa_N composition) in N-polar HEMT structures moves the charge centroid away from the interface. This behavior is similar to that in the Ga-polar HEMT structures. Therefore, in the last two mentioned cases, the 2DEG mobility first increases slightly as the n_s decreases, and decreases slightly at very low charge densities. It is also shown that SSDs have large impact on the 2DEG mobility only in the N-polar (Ga-polar) HEMTs with thin channels (barriers). *Published by AIP Publishing.* [<http://dx.doi.org/10.1063/1.4962321>]

INTRODUCTION

In recent years, Ga_N-based high-frequency high electron mobility transistors (HEMTs) structures have attracted much attention due to their high frequency and high power performances.^{6,19} N-polar HEMTs have several advantages over the traditional Ga-polar devices. The natural back-barrier in N-polar HEMTs improves the 2DEG confinement and leads to both lower output conductance and better pinch-off as well. To maintain a sufficient 2DEG density in either orientation, either a relatively thick Al(In)Ga_N or a very high Al composition Al(In)Ga_N charge inducing barrier layer is required. Because this barrier layer is located above the 2DEG (towards the surface) in the Ga-polar HEMTs, a trade-off exists between the charge density and the degree to which the barrier layer can be scaled.³⁴ This trade-off is mitigated in N-polar devices, allowing aggressive scaling of the transistor dimensions while maintaining a sufficiently high 2DEG density.^{21,22}

Both the RF and power switching performance of transistors improve with enhanced mobility.¹⁴ Therefore, it is important to understand the source of electron scattering in order to improve the device quality. Although the 2DEG mobility in the Ga-polar HEMT structures has been studied extensively,^{12,15,16,33} few works have been published on the calculation of the 2DEG mobility in the N-polar HEMT structures.^{1,4,28}

There are three different ways of reducing the charge density (n_s) in N-polar high electron mobility transistors (HEMT) structures: by decreasing the channel thickness (t_{ch}), applying a reverse gate bias (V_G), or modifying the back-barrier. Understanding the behaviour of the 2DEG mobility as a function of n_s is essential to design high performance HEMT devices. Experimental data show that in N-polar AlGa_N-Ga_N heterostructures, the 2DEG mobility reduces as n_s decreases. A decrease in channel thickness^{21,28} or an application of reverse bias⁴ to the gate results in a reduction of the 2DEG density (n_s) in addition to a reduction in the 2DEG mobility, which combine to give significantly higher sheet resistance, whereas in the Ga-polar HEMT structures, the 2DEG mobility increases as the n_s in the channel decreases by applying reverse gate bias.⁸ Brown *et al.*⁴ attributed the reduction in mobility with increasing reverse gate bias in N-polar heterostructures to alloy scattering. They claimed that by applying higher reverse gate bias, the electric field in the channel increases significantly, which leads to further penetration of 2DEG wavefunction into the alloy back-barrier and larger alloy scattering rate. In a separate work, Singiseti *et al.*²⁸ attributed the 2DEG mobility reduction in N-polar HEMT structure caused by decreasing the channel thickness to larger interface roughness scattering due to larger electric field. Our calculations revealed that although decreasing the channel thickness or increasing the

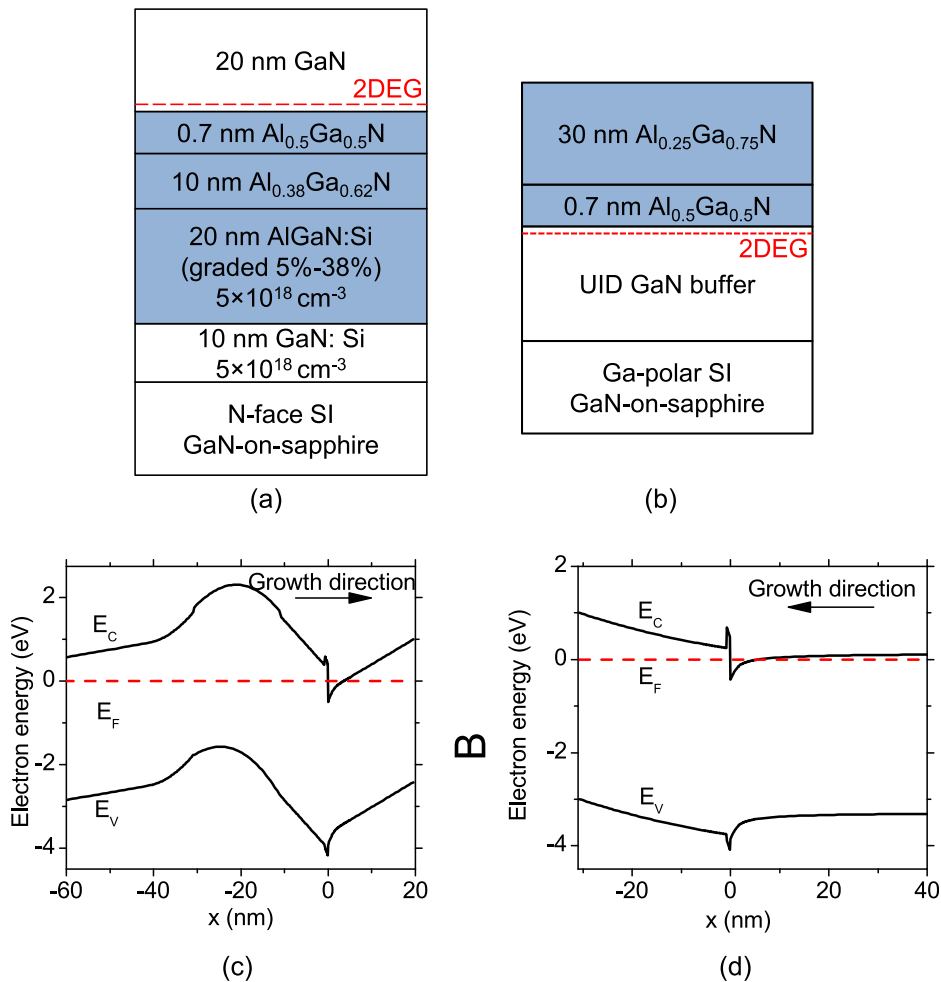


FIG. 1. Schematic of a typical (a) N-polar and (b) Ga-polar HEMT structures, with AlGa_N as the barrier, along with their corresponding band diagrams demonstrated in (c) and (d), respectively.

reverse gate bias in N-polar HEMTs increases interface roughness and alloy scattering rates, it is not significant enough to explain the severe reduction in the 2DEG mobility seen at room temperature (RT). We propose charged interface states (CIS) at the GaN-AlGa_N interface^{24,30} as the scattering mechanism responsible for the large reduction in the 2DEG mobility observed with decreasing channel thickness and/or increasing reverse gate bias in N-polar heterostructures. We also show that surface state dipoles (SSD) have a large effect in decreasing 2DEG mobility in thin channels where the dipoles are close to the 2DEG.

In this paper, we first discuss the procedure we used to calculate the 2DEG wavefunction needed for scattering rate calculations. Thereafter, we discuss the mobility limit associated with the conventional scattering mechanisms as well as CIS and SSD scatterings for the N- and Ga-polar HEMT structures at room temperature. The behavior of the 2DEG mobility is then demonstrated as a function of n_s and compared between the N- and Ga-polar HEMT structures.

PROCEDURE

We used the Born approximation to calculate the matrix elements of each perturbation potential.^{27,28} For an accurate evaluation of the scattering rates, the finite extent of the 2DEG perpendicular to its plane must be accounted for. The Fang-Howard variational wavefunction has been used for

this purpose in the past. However, this method does not consider the wavefunction penetration into the barrier. Thus, it is not a suitable approximation for the calculation of interface roughness or alloy disorder scattering. For this reason, a modified version of the Fang-Howard variational wavefunction has been developed,⁴ for which the electric field in the channel should be calculated first. Brown *et al.*⁴ estimated the electric field in the channel using the Poisson equation, while assuming that it is safe to ignore the Schrödinger correction. This resulted in an exaggeration of the effect of reverse bias on the electric field variation in the channel. Particularly, their approach overestimated the penetration of 2DEG into the barrier, and consequently, the effect of alloy scattering on the 2DEG mobility. Therefore, they attributed the 2DEG mobility reduction caused by applying reverse gate bias to larger alloy scattering rate. In this work, instead of using the above-mentioned approximation, we employed BandEng,¹¹ a 1D Poisson-Schrödinger self-consistent solver, to obtain the exact wavefunction.

The HEMT structures for which the calculations are performed are typical structures that are normally grown by metal organic chemical vapor deposition (MOCVD). There is an AlN interlayer between the GaN channel and the alloy barrier in a typical GaN-based HEMT structure to suppress the 2DEG penetration into the alloy barrier and improve the 2DEG mobility. However, it was discovered recently that the nominal AlN grown by MOCVD is, in practice, AlGa_N with

TABLE I. Si concentration in the graded-AlGa_N layer and AlN mole fraction in both graded-AlGa_N and the AlGa_N layer with constant composition were changed to tune in n_s in the N-polar HEMT structure shown in Fig. 1(a). The 7 Å of Al_{0.5}Ga_{0.5}N remained unaltered for all the structures.

n_s (cm ⁻³)	Si concentration (cm ⁻³)	AlN mole fraction
1.3×10^{13}	5×10^{18}	0.38
1.0×10^{13}	4×10^{18}	0.30
8.9×10^{12}	3×10^{18}	0.25
6.8×10^{12}	2×10^{18}	0.20
4.7×10^{12}	1×10^{18}	0.15
3.3×10^{12}	5×10^{17}	0.10

less than 50% AlN mole fraction for the Ga-polar HEMT structures.¹⁸ In this study, we assume that the unintentional Ga incorporation into N-polar AlN layer is the same. Therefore, to be as close as possible to the real structures, we assumed a 7 Å-thick Al_{0.5}Ga_{0.5}N as the interlayer in both the N-polar (Fig. 1(a)) and Ga-polar (Fig. 1(b)) HEMT structures. The corresponding band diagrams are shown in Figs. 1(c) and 1(d) for the N-polar and Ga-polar HEMT structures, respectively.

In the N-polar HEMT structures, there are three possible ways of reducing n_s in the channel, by either applying reverse gate bias, decreasing channel thickness, or modifying the back-barrier. As shown in Table I, the back-barrier was modified by changing the Si concentration in the graded-AlGa_N layer and the AlN mole fraction of both graded-AlGa_N and the AlGa_N layer with constant composition. The 7 Å-thick Al_{0.5}Ga_{0.5}N layer was kept unaltered. Figs. 2(a)–2(c) show the 2DEG wave-function, extracted from BandEng, near the channel in the N-polar HEMT structure

shown in Fig. 1(a) for different gate voltages, different channel thicknesses, and different back-barriers, respectively. As illustrated in these figures, for the first two cases, the charge centroid moves closer to the interface as the charge density decreases. In contrast, if n_s is reduced by modifying the back-barrier, the charge centroid moves away from the AlGa_N-Ga_N interface. This is similar to that in the Ga-polar HEMT structures (Fig. 2(d)). The distance between the charge centroid and the interface was calculated for all the cases and is shown in Fig. 3 for comparison.

Using the wavefunction exported from BandEng, the 2DEG mobility was then calculated through the Boltzmann transport equation in the relaxation time approximation. After calculating the mobility limited by each scattering mechanism, the Matthiessen rule was then applied to combine their influences and calculate the total RT 2DEG mobility.

SCATTERING MECHANISMS

All the commonly considered scattering mechanisms such as optical phonons, acoustic deformation potential, alloy, interface roughness, background ionized impurity (BII), remote ionized impurity (RII), and charged threading dislocations were included in our calculations.

Although the channel is not intentionally doped in GaN HEMTs, there is normally an n-type doping with a concentration of $\sim 1 \times 10^{16}$ cm⁻³ which comes from the unintentional oxygen incorporation in the layer during the epitaxial growth. Oxygen acts as a shallow donor in GaN. Unintentional background ionized (BII) impurities are a source of scattering.

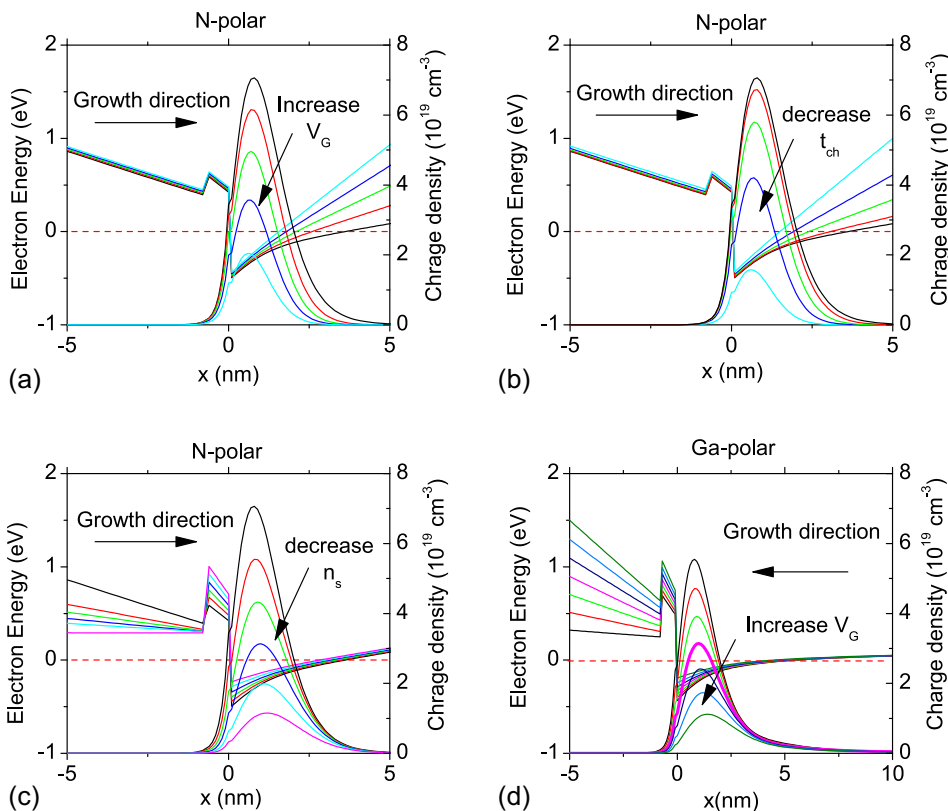


FIG. 2. 2DEG wavefunction along with the band diagram near the channel for the N-polar HEMT structure shown in Fig. 1(a) for (a) various V_G values ($t_{ch} = 20$ nm), (b) various channel thicknesses ($V_G = 0$ V), (c) back-barriers with different Si concentrations and AlGa_N compositions, and (d) Ga-polar HEMT structure shown in Fig. 1(b) for various V_G values. The charge centroid moves closer to the AlGa_N-Ga_N interface as n_s decreases for cases (a) and (b), whereas it moves away from the interface in cases (c) and (d).

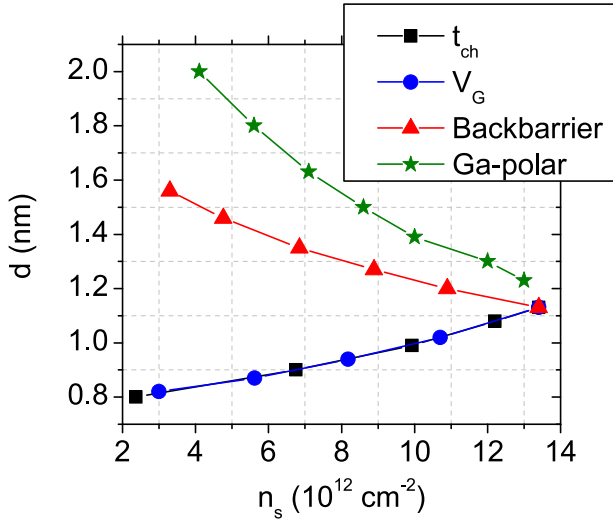


FIG. 3. Distance between the charge centroid and the AlGaIn-GaN interface as a function of n_s . The n_s in the N-polar HEMT was varied by either changing V_G (blue circles), changing t_{ch} (black squares), or modifying the back-barrier (red triangles). In the Ga-polar HEMT structure, n_s was changed by changing V_G (green stars).

In the GaN-based HEMTs, it is not necessary to dope the barrier in order to form 2DEG in the channel as opposed to the GaAs-based HEMTs. The polarization discontinuity at the interface is enough to induce a large sheet charge density in the channel.²⁹ Nevertheless, it has been demonstrated that doping the back-barrier in the N-polar HEMTs helps to reduce dispersion in the current-voltage characteristics.³² Therefore, as shown in Fig. 1(a), a part of AlGaIn back-barrier is usually Si-doped. The remote ionized impurities (RII) are also a source of scattering.

Because free-standing (FS) GaN substrates are presently cost-prohibitive for widespread use, the commercial GaN-based HEMTs are commonly grown heteroepitaxially on sapphire, Si, or SiC. Under optimized growth conditions on these materials, threading dislocation density (TDD) of epitaxial GaN layers is typically around $\sim 3 \times 10^8$ cm⁻². The charge accumulation along dislocations and the resulting electric field scatters the 2DEG wavefunction.^{16,31}

Although BII, RII, and TDD scattering mechanisms in addition to interface roughness scattering limit the 2DEG mobility at low temperature (where phonon scattering is negligible), the mobility limit considering all of them is more than 1×10^5 cm²/V s, and therefore do not play a significant role in limiting the RT 2DEG mobility. Furthermore, our calculations confirmed that 7 Å of Al_{0.5}Ga_{0.5}N presents a large enough barrier height to suppress the wavefunction penetration into the alloy barrier. The probability of wavefunction penetration into the Al_{0.5}Ga_{0.5}N barrier remained below 6% for all the cases. Therefore, the mobility limited by only alloy scattering was more than 1×10^5 cm²/V s for all cases. Note that assuming a pure AlN interlayer would decrease the wavefunction penetration into the barrier and hereby not affect the conclusion of this paper. While the abovementioned scattering mechanisms are included in our calculations, we do not delve into the details of calculations, and one can refer to the available literature^{2,5,16} for more details.

Phonon scattering

Phonons scatter electrons through coupling to both deformation as well as piezoelectric potentials in polar materials. In the GaN HEMTs, polar optical phonon scattering is typically the dominant scattering mechanism at room temperature. However, polar acoustic phonon (known as piezoelectric scattering) is negligible in comparison to the acoustic deformation potential scattering. Furthermore, although acoustic phonons have both longitudinal and transverse components, the transverse mode can be safely ignored as it is much weaker than the longitudinal mode.²³ Therefore, we only included polar optical phonon and acoustic deformation potential in our calculations.

The relaxation time approximation is only applicable to describe elastic scattering events, whereas phonon scattering is an inelastic mechanism. Regardless, since the acoustic phonon energy is very low, it is safe to treat it as an elastic scattering, and the scattering rate can be defined as⁵

$$\frac{1}{\tau_{AC}} = \frac{m^* a_c^2 k_B T}{\rho v_s^2 \hbar^3} I, \quad (1)$$

where ρ , v_s , and a_c are mass density, sound velocity, and the deformation potential of GaN. k_B is the Boltzmann constant. The dependence of acoustic scattering on the width of the 2DEG wavefunction manifests itself through parameter $I = \int_{-\infty}^{+\infty} |\psi(z)|^2 |\psi(z)|^2 dz$ in Eq. (1).⁵ The RT 2DEG mobility limited only by acoustic deformation potential scattering was calculated for the N- and Ga-polar HEMT structures as a function of n_s , and the results are shown in Fig. 4. The RT mobility limited by acoustic phonon decreases as n_s is decreased by applying V_G or reducing t_{ch} in the N-polar HEMT structure. This is due to higher confinement of wavefunction in channel as n_s is reduced in these two cases. On the contrary, in the case that n_s is altered by modifying the back-barrier, the wavefunction widens as n_s is reduced. A similar behavior was observed in Ga-polar HEMT structures.

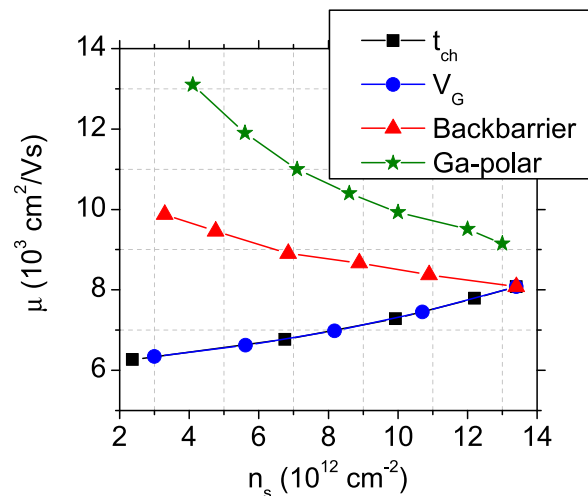


FIG. 4. RT 2DEG mobility limited by acoustic phonon as a function of n_s . The n_s in the N-polar HEMT was varied by either changing V_G (blue circles), changing t_{ch} (black squares), or modifying the back-barrier (red triangles). In the Ga-polar HEMT structure, n_s was changed by changing V_G (green stars).

The mobility limited by acoustic phonon increases as n_s decreases in the last two cases.

Optical phonons in GaN have high energy (90 meV). In 1993, Gelmont *et al.*⁹ introduced an analytical approach to calculate the optical phonon momentum relaxation time in the case of wide bandgap semiconductors, such as GaN, for which the optical phonon energy is much larger than $k_B T$. In these types of semiconductors, because the optical phonon energy is much larger than the electron's thermal energy (even at room temperature), the probability for phonon absorption is much higher than phonon emission. Therefore, the momentum relaxation time can be derived considering only phonon absorption. Moreover, in 1994,¹⁰ it was shown by the same authors that when the sub-band levels are close to each other (the difference is smaller than optical phonon energy), the scattering rate of optical phonon in 2DEG can be estimated using the scattering rate of optical phonons in the bulk. This is specifically true for GaN since optical phonons have relatively large energy in this material system. Using the material parameters for GaN, the RT mobility limited by optical phonons in bulk GaN was calculated to be $2400 \text{ cm}^2/\text{V s}$.

Before proceeding with other scattering mechanisms, it is worth paying close attention to the RT 2DEG mobility in an ideal GaN-based HEMT structure where all the scattering mechanisms are absent, and the 2DEG mobility is limited only by crystal vibrations (acoustic and optical phonons). In that case, the RT 2DEG mobility was calculated to be $1745 \text{ cm}^2/\text{V s}$ and $1900 \text{ cm}^2/\text{V s}$ in the N- and Ga-polar HEMTs, respectively, given by $1/\mu(300 \text{ K}) = 1/\mu_{OP}(300 \text{ K}) + 1/\mu_{AC}(300 \text{ K})$. These values are lower than the record electron mobility values reported in the literature.^{17,20} We speculate that this is due to the overestimation of the deformation coupling constant in acoustic scattering. This could be attributed to the deformation-related variation of effective mass, which is negligible in bulk. The variation of effective mass could reduce the effective coupling constant for 2DEG in comparison to that in bulk GaN.^{25,26}

Surface state dipoles

As it was discussed previously, there is a large polarization charge at the AlGaIn-GaN interface. This bound polarization is only partially compensated by the formation of the 2DEG in the channel, and the rest of it is compensated by the charged surface states. Although the nature of these surface states is not yet well-understood, extensive dangling bonds, vacancies at the surface, and oxidation have been suggested as the origin of such states.⁷ These charged surface states similar to remote ionized impurities scatter electrons in the 2DEG. In the case of the N-polar HEMT structures, a dielectric (usually SiN) is deposited on the surface before fabricating transistor patterns to protect the surface from being etched in the developer. Therefore, instead of a sheet of positive charges, there is a sheet of dipoles on the surface as shown in Fig. 5.

The formula to calculate the scattering rate from SSDs was derived using a superposition of positive and negative charges and is given by

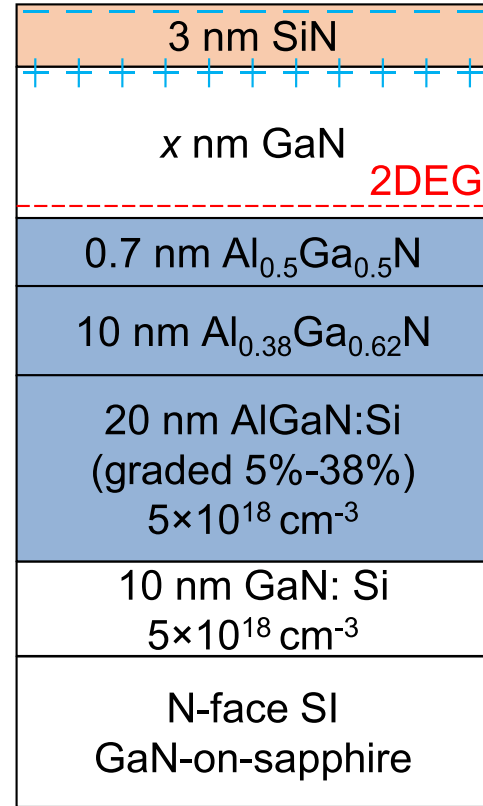


FIG. 5. Schematic of a typical N-polar HEMT structure showing the SiN dielectric and surface state dipoles.

$$\frac{1}{\tau_{SSD}} = N_{SSD} \frac{m^*}{2\pi\hbar^3 k_F^3} \left(\frac{e^2}{\epsilon_0 \epsilon_r} \right) \times \int_0^{2k_F} dq \frac{F(q) e^{-2qt_{ch}} \sinh\left(\frac{qt_{SiN}}{2}\right)}{(q + q_{TF} G(q))^2} \cdot \frac{q^2}{\sqrt{1 - \left(\frac{q}{2k_F}\right)^2}}, \quad (2)$$

where t_{SiN} and t_{ch} are the dielectric and channel thicknesses (barrier thickness in the case of the Ga-polar HEMTs), respectively, and N_{SSD} is the density of surface state dipoles. The 2DEG mobility limited by SSDs was calculated as a function of n_s for both the N- and Ga-polar HEMT structures, and the results are shown in Fig. 6. The density of surface state dipoles was assumed to be $2 \times 10^{12} \text{ cm}^{-2}$ in our calculations.⁷ These calculations revealed that SSDs have an impact on the 2DEG mobility only when they are close to the 2DEG.

The density of SSDs depends strongly on the growth and processing conditions. The 2DEG mobility including all the scattering mechanisms was calculated as a function of N_{SSD} for the N-polar HEMT structure with 5 nm-thick GaN channel ($n_s = 2 \times 10^{12} \text{ cm}^{-2}$). As demonstrated in Fig. 7, the 2DEG mobility is independent of SSDs for N_{SSD} lower than $4 \times 10^{11} \text{ cm}^{-2}$.

The scattering rate decays exponentially as the distance between surface state dipoles and channel increases (Eq. (2)), implying that the surface state dipoles have an impact on the 2DEG mobility only in the N-polar (Ga-polar) HEMTs with thin channels (barriers).

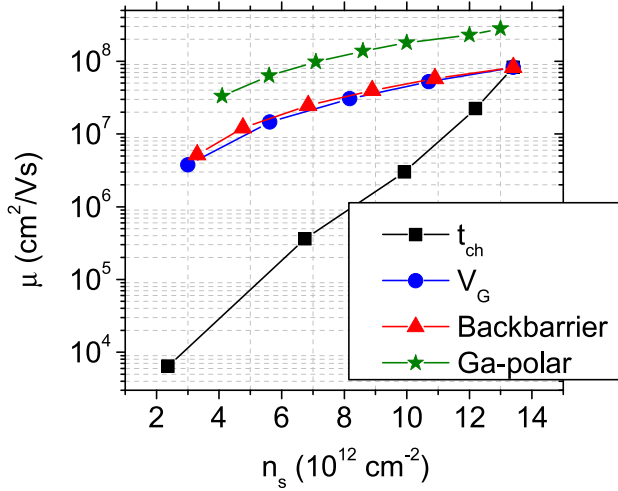


FIG. 6. RT 2DEG mobility limited by surface state dipoles as a function of n_s . A N_{SSD} of $2 \times 10^{12} \text{ cm}^{-2}$ was assumed in these calculations. The n_s in the N-polar HEMT was varied by either changing V_G (blue circles), changing t_{ch} (black squares), or modifying back-barrier (red triangular). In the Ga-polar HEMT structure, n_s was changed by changing V_G (green stars).

Charge states at the AlGaIn-GaN interface

The conductance method was first proposed by Haddara and El-Sayed¹³ to measure the trap state between the Si-SiO₂ interface. This method was later adopted by Miller *et al.*²⁴ to measure the trap state at the GaN-AlGaIn interface in the Ga-polar GaN/AlGaIn heterostructure. They reported an interface state density of $1 \times 10^{12} \text{ cm}^{-2}$ with an energy of 0.3 eV below the conduction band. Recently, Waller *et al.*³⁰ showed that using the conductance method for extracting interface states is valid only for HEMTs with short gate length ($L_G < 10 \mu\text{m}$). Utilizing this method for HEMTs with long gate lengths results in exaggerated interface state density. Waller *et al.*³⁰ measured an interface state density of $5 \times 10^{10} \text{ cm}^{-2}$ in the Ga-polar GaN/AlGaIn HEMTs which had gate lengths lower than $10 \mu\text{m}$. The reason behind the formation of these interface states is not well-understood yet. They could be attributed to AlGaIn-GaN intermixing at the interface or oxygen unintentionally incorporated into the AlGaIn layer.

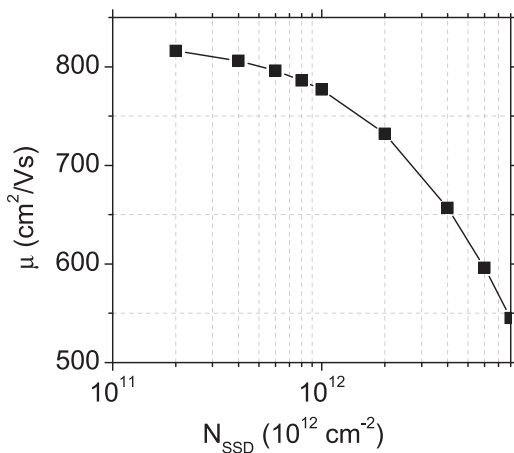


FIG. 7. RT 2DEG mobility as a function of N_{SSD} for N-polar HEMT structures with $t_{ch} = 5 \text{ nm}$.

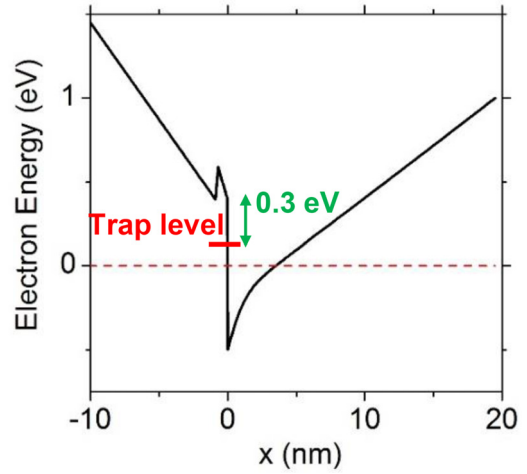


FIG. 8. Band diagram of the N-polar HEMT structure showing interface trap state at the AlGaIn-GaN interface.

As shown in Fig. 8, these trap states are above the Fermi level and, therefore, depleted and positively charged. The charged states can be modeled similar to remote ionized impurity for the purpose of the 2DEG mobility calculations. The CIS scattering rate is then given by

$$\frac{1}{\tau_{CIS}} = N_{CIS} \frac{m^*}{2\pi\hbar^3 k_F^3} \left(\frac{e^2}{2\epsilon_0\epsilon_s} \right)^2 \int_0^{2k_F} dq \frac{F(q)}{(q + q_{TF}G(q))^2} \times \frac{\exp(-2qd)q^2}{\sqrt{1 - \left(\frac{q}{2k_F}\right)^2}}, \quad (3)$$

where a sheet of positive charge with a density of N_{CIS} was assumed at the AlGaIn/GaN interface. d is the distance between the charge centroid and the AlGaIn/GaN interface.

The 2DEG mobility limited by CISs was calculated as a function of n_s for both the N- and Ga-polar HEMT structures shown in Figs. 1(a) and 1(b), respectively. A CIS density of $8 \times 10^{11} \text{ cm}^{-2}$ was assumed for these calculations. The results are shown in Fig. 9. The mobility limited by CISs drops as the charge density decreases. This mobility drop is due to less screening of the scattering potential by 2DEG as the charge density decreases. It is important to note that in the N-polar HEMT structures, for the cases that n_s is decreased by applying reverse gate bias or reducing the channel thickness (Fig. 9, black squares and blue circles), the 2DEG mobility limited by CIS drops much sharper than when n_s is reduced by modifying the back-barrier (Fig. 9, red triangular). The reason is that in the first two cases, d decreases with decreasing n_s , whereas in the latter case, d increases (similar to Ga-polar HEMT structures). From Eq. (3), the scattering rate decays exponentially as the distance between the 2DEG centroid and the interface increases. Figure 10 shows 2DEG mobility as a function of density of CISs. The calculations were performed for the N-polar HEMT structure shown in Fig. 1(a) with $V_G = -4 \text{ V}$.

2DEG MOBILITY AND DISCUSSION

The RT 2DEG mobility was calculated using the Matthiessen rule considering all the above-mentioned

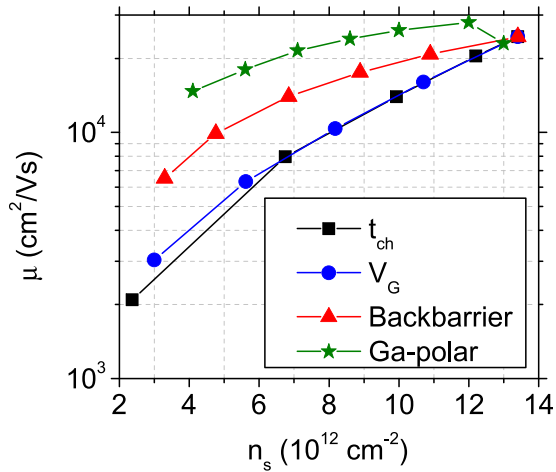


FIG. 9. RT 2DEG mobility limited by the AlGaIn-GaN interface states as a function of n_s . An N_{CIS} of $8 \times 10^{11} \text{ cm}^{-2}$ was assumed for these calculations. The n_s in N-polar HEMT was varied by either changing V_G (blue circles), changing t_{ch} (black squares), or modifying back-barrier (red triangular). In the Ga-polar HEMT structure, n_s was changed by changing V_G (green stars).

scattering mechanisms, and the results are demonstrated in Fig. 11. Our calculations suggest that in the N-polar HEMT structures, the behavior of the 2DEG mobility as a function of n_s depends on the method applied to reduce n_s . In the cases where n_s is reduced by applying reverse gate bias or decreasing the channel thickness, the 2DEG mobility drops sharply by reducing n_s . On the other hand, if n_s is reduced by modifying the back-barrier, the 2DEG mobility slightly improves as n_s decreases, and drops slightly at very low charge densities. These different trends can be justified by looking at the distance between the charge centroid and the AlGaIn-GaN interface (Fig. 3). In the former case, the charge centroid moves closer to the interface by reducing n_s , whereas in the latter case, it moves away from the interface. Similarly, in the Ga-polar HEMT structures, where n_s is reduced by applying reverse gate bias, the charge centroid moves away from the

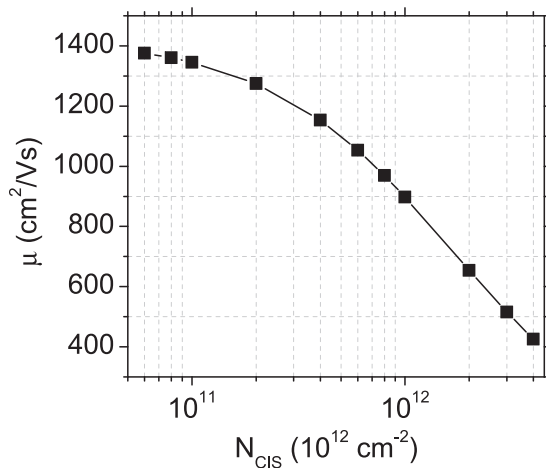
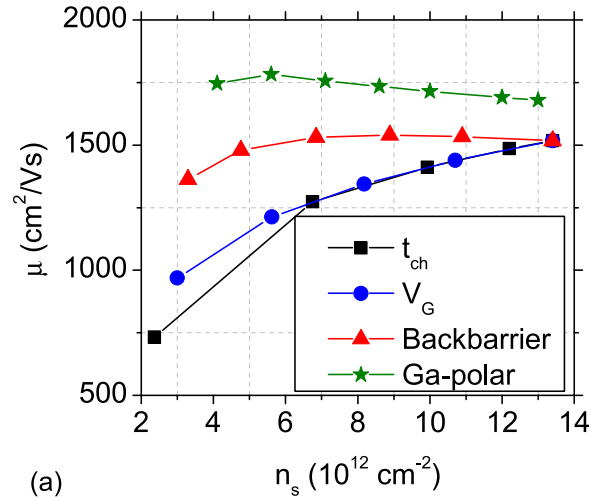
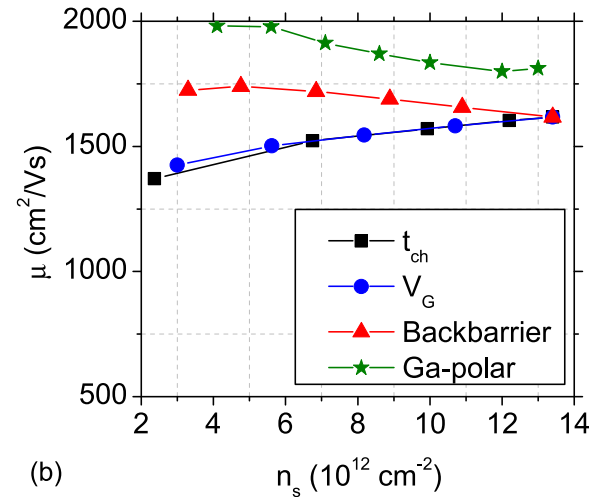


FIG. 10. RT 2DEG mobility as a function of N_{CIS} for the N-polar HEMT structure shown in Fig. 1(a) with $V_G = -4\text{V}$.



(a)



(b)

FIG. 11. RT 2DEG mobility as a function of n_s including (a) all scattering mechanisms and (b) only conventional scattering mechanisms. N_{CIS} and N_{SSD} of $8 \times 10^{11} \text{ cm}^{-2}$ and $2 \times 10^{12} \text{ cm}^{-2}$, respectively, were assumed for these calculations. The n_s in the N-polar HEMT was varied by either changing V_G (blue circles), changing t_{ch} (black squares), or modifying the back-barrier (red triangular). In the Ga-polar HEMT structure, n_s was changed by changing V_G (green stars).

interface. Therefore, the 2DEG mobility as a function of n_s should follow a similar trend to that in the N-polar HEMT structures where n_s is reduced by modifying the back-barrier. This was confirmed by our calculations.

To understand the importance of scattering from CISs and SSDs, the 2DEG mobility for all the above-mentioned cases was calculated considering only conventional scattering mechanisms (Fig. 11(b)). Our calculations revealed that conventional scattering mechanisms by themselves cannot explain the 2DEG mobility dependence on n_s either in the Ga-polar⁸ or N-polar^{3,4,28} HEMT structures.

Previously, it was believed that increasing the reverse gate bias or decreasing the channel thickness in the N-polar GaN-based HEMT structures lead to deeper penetration of the 2DEG wavefunction into the barrier and, consequently, higher interface roughness and alloy scattering rates. Our calculations revealed that the penetration of the 2DEG into

the barrier and, therefore, the 2DEG mobility limited by alloy and interface roughness scattering mechanisms do not vary significantly by increasing the reverse gate bias or decreasing the channel thickness. Therefore, these two scattering mechanisms alone cannot explain the significant drop in the 2DEG mobility observed in experiments. Rather, our calculations demonstrate that the charged states at the AlGaIn/GaN interface are responsible for the large reduction in the 2DEG mobility seen with increasing reverse gate bias and decreasing channel thickness. Furthermore, for very thin channels in the N-polar HEMTs and thin barrier layers in the Ga-polar HEMTs, scattering from SSDs has a large impact on reducing the 2DEG mobility.

SUMMARY

In summary, we introduced scattering from the charged interface states to explain the dependence of the 2DEG mobility to charge density in the channel observed from experimental data in both the N-polar and Ga-polar HEMT structures. We showed that the 2DEG mobility as a function of n_s has a similar behavior for cases where n_s is reduced by applying reverse gate bias or decreasing channel thickness. In both cases, the mobility drops severely as the charge density decreases. On the contrary, for the case where n_s is reduced by modifying the back-barrier, first the 2DEG mobility slightly improves as the n_s decreases, and it drops slightly for very small charge densities. This behavior is similar to that observed in the Ga-polar HEMT structures. We showed that this difference is attributed to the distance between the charge centroid and the AlGaIn-GaN interface. In the former case, the charge centroid moves closer to the interface as n_s decreases, whereas in the latter case, it moves away from the interface, which leads to less scattering from CISs. In addition, we showed that SSDs have a large impact on the 2DEG mobility only in the N-polar (Ga-polar) HEMTs with thin channels (barriers).

ACKNOWLEDGMENTS

The authors would like to acknowledge funding support from the Office of Naval Research (Dr. P. Maki, Program Manager).

¹E. Ahmadi, H. Chalabi, S. W. Kaun, R. Shivaraman, J. S. Speck, and U. K. Mishra, "Contribution of alloy clustering to limiting the two-dimensional electron gas mobility in AlGaIn/GaN and InAlN/GaN heterostructures: Theory and experiment," *J. Appl. Phys.* **116**(13), 133702 (2014).

²G. Bastard, *Wave Mechanics Applied to Semiconductor Heterostructures* (Les Editions de Physique, 1988).

³D. F. Brown, "Growth of nitrogen-polar gallium nitride-based materials and high electron mobility transistors by metal organic chemical vapor deposition," Ph.D. thesis, UC-Santa Barbara, 2010.

⁴D. F. Brown, S. Rajan, S. Keller, Y.-H. Hsieh, S. P. DenBaars, and U. K. Mishra, "Electron mobility in N-polar GaN/AlGaIn/GaN heterostructures," *Appl. Phys. Lett.* **93**(4), 042104 (2008).

⁵J. H. Davies, *The Physics of Low-dimensional Semiconductors: An Introduction* (Cambridge University Press, 1998).

⁶D. Denninghoff, J. Lu, E. Ahmadi, S. Keller, and U. K. Mishra, "N-polar GaN/InAlN/AlGaIn MIS-HEMTs with 1.89 S/mm extrinsic transconductance, 4 A/mm drain current, 204 GHz f_T and 405 GHz f_{max} ," in *71st Annual Device Research Conference (DRC)* (IEEE, Piscataway, NJ, USA, 2013), pp. 197–198.

⁷B. S. Eller, J. Yang, and R. J. Nemanich, "Electronic surface and dielectric interface states on GaN and AlGaIn," *J. Vac. Sci. Technol., A* **31**(5), 050807 (2013).

⁸R. Gaska, M. S. Shur, A. D. Bykhovski, A. O. Orlov, and G. L. Snider, "Electron mobility in modulation-doped AlGaIn-GaN heterostructures," *Appl. Phys. Lett.* **74**(2), 287 (1999).

⁹B. Gelmont, K. Kim, and M. Shur, "Monte carlo simulation of electron transport in gallium nitride," *J. Appl. Phys.* **74**(3), 1818–1821 (1993).

¹⁰B. L. Gelmont, M. Shur, and M. Stroschio, "Polar optical-phonon scattering in three- and two-dimensional electron gases," *J. Appl. Phys.* **77**(2), 657–660 (1995).

¹¹M. Grundmann, BandEng; available at <http://my.ece.ucsb.edu/mgrundmann/bandeng/>.

¹²M. Gurusinge, S. Davidsson, and T. Andersson, "Two-dimensional electron mobility limitation mechanisms in $Al_xGa_{1-x}N$ /GaN heterostructures," *Phys. Rev. B* **72**(4), 045316 (2005).

¹³H. S. Haddara and M. El-Sayed, "Conductance technique in MOSFETs: Study of interface trap properties in the depletion and weak inversion regimes," *Solid-State Electron.* **31**(8), 1289–1298 (1988).

¹⁴A. Q. Huang, "New unipolar switching power device figures of merit," *IEEE Electron Device Lett.* **25**(5), 298–301 (2004).

¹⁵D. Jena, I. Smorchkova, A. C. Gossard, and U. K. Mishra, "Electron transport in iii-v nitride two-dimensional electron gases," *Phys. Status Solidi B* **228**(2), 617–619 (2001).

¹⁶D. Jena, A. C. Gossard, and U. K. Mishra, "Dislocation scattering in a two-dimensional electron gas," *Appl. Phys. Lett.* **76**(13), 1707 (2000).

¹⁷S. W. Kaun, P. G. Burke, M. H. Wong, E. C. H. Kyle, U. K. Mishra, and J. S. Speck, "Effect of dislocations on electron mobility in AlGaIn/GaN and AlGaIn/AlN/GaN heterostructures," *Appl. Phys. Lett.* **101**(26), 262102 (2012).

¹⁸S. W. Kaun, B. Mazumder, M. N. Fireman, E. C. H. Kyle, U. K. Mishra, and J. S. Speck, "Pure AlN layers in metal-polar AlGaIn/AlN/GaN and AlN/GaN heterostructures grown by low-temperature ammonia-based molecular beam epitaxy," *Semicond. Sci. Technol.* **30**(5), 055010 (2015).

¹⁹S. Kolluri, S. Keller, S. P. DenBaars, and U. K. Mishra, "N-Polar AlGaIn/GaN MIS-HEMTs on SiC with a 16.7 W/mm power density at 10 GHz using an Al_2O_3 based etch stop technology for the gate recess," in *69th Annual Device Research Conference (DRC)* (IEEE, Piscataway, NJ, USA, 2011), pp. 2015–2016.

²⁰H. Li, S. Keller, S. H. Chan, J. Lu, S. P. DenBaars, and U. K. Mishra, "Unintentional gallium incorporation in AlN and its impact on the electrical properties of GaN/AlN and GaN/AlN/AlGaIn heterostructures," *Semicond. Sci. Technol.* **30**(5), 055015 (2015).

²¹J. Lu, D. Denninghoff, R. Yeluri, S. Lal, G. Gupta, M. Laurent, S. Keller, S. P. DenBaars, and U. K. Mishra, "Very high channel conductivity in ultra-thin channel N-polar GaN/(AlN, InAlN, AlGaIn) high electron mobility hetero-junctions grown by metalorganic chemical vapor deposition," *Appl. Phys. Lett.* **102**(23), 232104 (2013).

²²J. Lu, X. Zheng, M. Guidry, D. Denninghoff, E. Ahmadi, S. Lal, S. Keller, S. P. DenBaars, and U. K. Mishra, "Engineering the (In, Al, Ga)N back-barrier to achieve high channel-conductivity for extremely scaled channel-thicknesses in N-polar GaN high-electron-mobility-transistors," *Appl. Phys. Lett.* **104**(9), 092107 (2014).

²³M. Lundstrom, *Fundamentals of Carrier Transport* (Cambridge University Press, 2009).

²⁴E. J. Miller, X. Z. Dang, H. H. Wieder, P. M. Asbeck, E. T. Yu, G. J. Sullivan, and J. M. Redwing, "Trap characterization by gate-drain conductance and capacitance dispersion studies of an AlGaIn/GaN heterostructure field-effect transistor," *J. Appl. Phys.* **87**(11), 8070–8073 (2000).

²⁵V. V. Mitin, V. I. Pipa, and M. A. Stroschio, "Contribution of effective mass variation to electro-acoustic phonon interaction in semiconductor nanostructures," *Microelectron. Eng.* **47**(1), 373–375 (1999).

²⁶V. I. Pipa, N. Z. Vagidov, V. V. Mitin, and M. Stroschio, "Electron-acoustic phonon interaction in semiconductor nanostructures: Role of deformation variation of electron effective mass," *Phys. Rev. B* **64**(23), 235322 (2001).

²⁷H. Sakaki, T. Noda, K. Hirakawa, M. Tanaka, and T. Matsusue, "Interface roughness scattering in GaAs/AlAs quantum wells," *Appl. Phys. Lett.* **51**(23), 1934 (1987).

²⁸U. Singiseti, M. H. Wong, and U. K. Mishra, "Interface roughness scattering in ultra-thin n-polar GaN quantum well channels," *Appl. Phys. Lett.* **101**(1), 012101 (2012).

- ²⁹I. P. Smorchkova, C. R. Elsass, J. P. Ibbetson, R. Vetry, B. Heying, P. Fini, E. Haus, S. P. Denbaars, J. S. Speck, and U. K. Mishra, "Polarization-induced charge and electron mobility in AlGa_N/Ga_N heterostructures grown by plasma-assisted molecular-beam epitaxy," *J. Appl. Phys.* **86**(8), 4520–4526 (1999).
- ³⁰W. M. Waller, S. Karboyan, M. J. Uren, K. B. Lee, P. Houston, D. J. Wallis, I. Guiney, C. J. Humphreys, M. Kuball *et al.*, "Interface state artefact in long gate-length AlGa_N/Ga_N HEMTs," *IEEE Trans. Electron Devices* **62**(8), 2464 (2015).
- ³¹N. G. Weimann, L. F. Eastman, D. Doppalapudi, H. M. Ng, and T. D. Moustakas, "Scattering of electrons at threading dislocations in Ga_N," *J. Appl. Phys.* **83**(7), 3656–3659 (1998).
- ³²M. H. Wong, U. Singisetti, J. Lu, J. S. Speck, and U. K. Mishra, "Anomalous output conductance in n-polar Ga_N high electron mobility transistors," *IEEE Trans. Electron Devices* **59**(11), 2988–2995 (2012).
- ³³D. Zanato, S. Gokden, N. Balkan, B. K. Ridley, and W. J. Schaff, "The effect of interface-roughness and dislocation scattering on low temperature mobility of 2d electron gas in Ga_N/AlGa_N," *Semicond. Sci. Technol.* **19**(3), 427 (2004).
- ³⁴Y. Zhang, I. P. Smorchkova, C. R. Elsass, S. Keller, J. P. Ibbetson, S. Denbaars, U. K. Mishra, and J. Singh, "Charge control and mobility in AlGa_N/Ga_N transistors: Experimental and theoretical studies," *J. Appl. Phys.* **87**(11), 7981 (2000).